

# SEISMIC BEHAVIOR AND ASSESSMENT OF CIRCULAR CONCRETE COLUMNS REINFORCED BY ULTRA-HIGH STRENGTH REBARS

Grigor SARGSYAN<sup>\*1</sup>, Yutaro TANAKA<sup>\*2</sup>, Takashi TAKEUCHI<sup>\*3</sup> and Yuping SUN<sup>\*4</sup>

## ABSTRACT

Four circular columns with diameter of 250mm were tested under combined reversed cyclic lateral force to investigate the seismic behavior of circular concrete columns partially confined by bolted thin steel plates with the aim of developing earthquake-resilient concrete columns. The main experimental variables were the confinement method and axial load level. Test results have indicated that the partial confinement by bolted thin steel plates could assure circular concrete columns subjected to a high axial compression with axial load ratio of 0.50 of sufficient resilience till drift angle of 0.04 rad.

**Keywords:** Circular column; Resilience; Steel plate confinement; Low residual deformation

## 1. INTRODUCTION

During the last twenty years, Japan has experienced two great earthquake disasters; the 1995 Kobe earthquake and the 2011 Tohoku earthquake. One of the most severe aftermath of these strong earthquakes is the cost of recovery. Based on the lessons learnt from these earthquakes, currently it is increasingly accepted that buildings and infra-structures must be safe not only during an earthquake but also after. Furthermore, from the viewpoint of prompt post-earthquake recovery of society and daily lives, assuring reliable usability and reparability of building structures that may be hit by potential mega-earthquakes such as the Nankai-trough earthquake is of significant importance. The resilience, which means recoverability of a structural member or component after earthquake and can be defined in terms of second tangent stiffness and residual deformation, becomes one of the important requirements that new buildings are supposed to meet.

The utilization of high strength materials in the construction field is a simple and effective method to make resilient concrete components due to their physical and mechanical properties. In order to ensure concrete columns, in particular the columns located at lower stories of a high-rise building, of sufficient resilience, the authors have suggested combination of confinement by bolted steel plates and replacement of longitudinal steels with ultra-high strength rebars in concrete columns. Efficacy of confinement by steel tubes or steel plates in improving ductility of concrete columns have previously been experimentally and analytically studied by several authors [1-4], all of which focused on evaluating the effectiveness of steel plate jackets as a seismic retrofit technique for

non-ductile rectangular or circular columns. As to the effectiveness of ultra-high strength rebars in enhancing resilience of circular concrete columns, it has been experimentally verified by Sun et al. as described in references 5 through 8.

These previous studies, however, dealt mainly with the performance of concrete columns with shear span ratio of about 2.0 and under double curvature deformation, which is common in story-failure building structures. In fact, due to the influence of higher vibration mode, the contra-flexure point in the columns located at the lower stories of a high-rise building tends to shift from the well-assumed middle height towards the upper end of the columns, resulting in enlargement of shear span ratio and premature degradation of load-carrying capacity due to the P- $\Delta$  effect at large deformation. Therefore, to promote application of the proposed combination into actual buildings, seismic performance of concrete columns with larger shear span ratio needs to be clarified.

The objectives of this study are to present some information on the effectiveness of confinement by bolted steel plates and using ultra-high strength rebars in enhancing resilience of circular columns with shear span ratio of 4.0, and to investigate effect of the type of longitudinal rebars on overall seismic behavior of circular concrete columns under high axial load.

## 2. EXPERIMENTAL PROGRAM

### 2.1. Outlines of The Test Columns

Four 1/3 scale cantilever circular concrete columns were designed, constructed and tested under constant axial compression and reversed cyclic lateral load. Fig. 1 and Table 1 show reinforcement details and outlines

\*1 Graduate School of Engineering, Kobe University, JCI Student Member

\*2 Graduate School of Engineering, Kobe University.

\*3 Assistant Professor, Graduate School of Engineering, Kobe University, JCI Member

\*4 Professor, Graduate School of Engineering, Kobe University, JCI Member

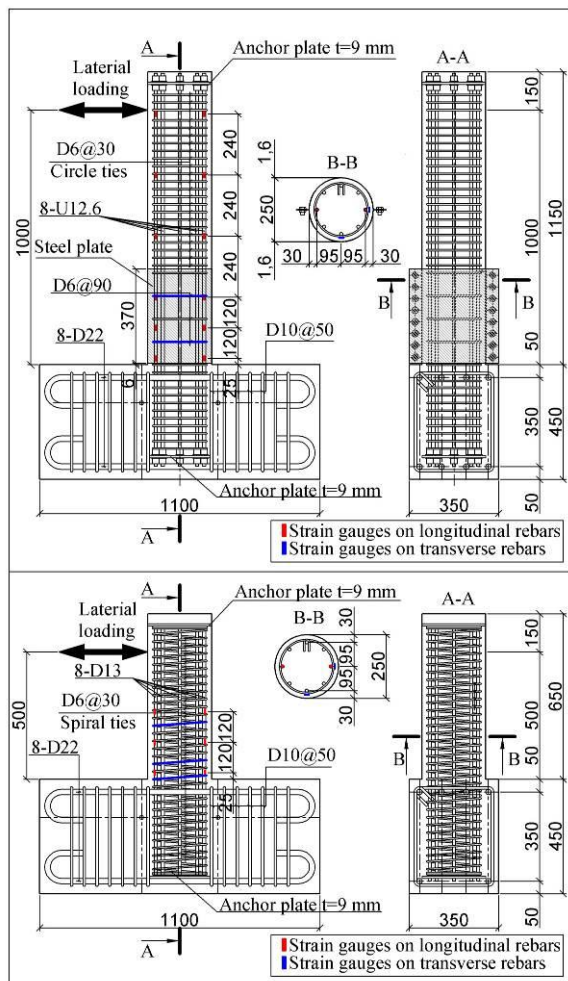


Fig. 1 Geometry of test columns (unit: mm)

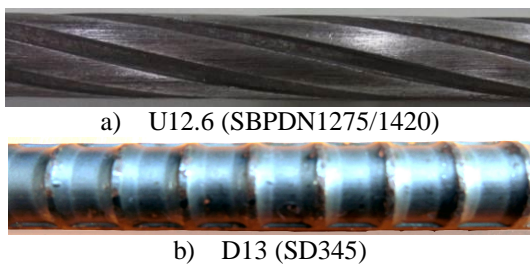


Fig. 2 Surface shapes of rebars

of the test specimens, respectively. The experimental parameters were shear span ratio (2.0 and 4.0), confinement method, and type of longitudinal rebars. As shown in Fig.1 and Table 1, one column was longitudinally reinforced by eight normal-strength D13 deformed rebars (SD345), and the other three columns by eight ultra-high strength U12.6 (SBPDN1275/1420) rebars. As shown in Fig. 2, the U12.6 rebar has spiraled grooves on its surface and a low bond-strength of about  $3.0\text{N/mm}^2$ , which is about one-fifth of that of D13 rebar as verified by Funato et al. [9].

Two columns with shear span ratio of 2.0 were confined by conventional D6 spiral with spacing of 30mm, while the columns with shear span ratio of 4.0 were partially confined by steel plates. As obvious from Fig. 1, only the end 1.5D ( $D = \text{depth of column section}$ ) region of the longer columns was wrapped by two

pieces of semi-circular shape of 1.6mm steel plates that are connected through bolts, and the bare-left region was confined by circular hoops with spacing of 30mm. The steel plates were bolted together before casting concrete, and hence worked as a form for the columns. To prevent the steel plates from directly sustaining axial stress induced by external moment and axial load, clearance of 6mm was provided between the lower end of steel plates and the top end of the stub for loading.

To simulate the columns located at lower stories of high-rise buildings, two high levels of axial load were set for the test columns. The axial load ratios were 0.33 and 0.50. The former corresponds to the upper limit recommended in current Japanese design standards [10] for general concrete columns, and the latter represents a potential axial load level which may occur in the corner columns of high-rise buildings when hit by a severe earthquake.

## 2.2. Material Properties

Ready-mixed concrete made of Portland cement and coarse aggregates with maximum particle size of 20mm was used to fabricate the specimens. The concrete strength shown in Table 1 represents the average value of three cylinders (100mm in diameter and 200mm in height). Mechanical properties of the steels used are listed in Table 2.

## 2.3. Test Setup and Loading Program

The test apparatus shown in Fig. 3 was used to apply in-plane lateral and axial loads. The constant axial compression was at first applied through a hydraulic jack of 1000kN in capacity, and then a hydraulic jack with capacities of 300kN in pulling and 500kN in pushing was used to apply the lateral force. The cyclical lateral force was controlled by drift ratio  $R$ , which is the ratio of lateral tip displacement to the shear span ( $a = 500\text{mm}$  or  $1000\text{mm}$ ). Two complete cycles were performed at each level of lateral displacement until drift ratio reached 0.02 rad, while beyond that drift level only one cycle was performed.

One displacement transducer (DT) was adopted to measure the tip lateral displacement and four DTs were installed to measure the overall axial displacement and local axial displacement within the end 1.5D region of the longer columns. Strain gauges were installed on two longitudinal rebars which located at the tensile and compressive sides of each column to measure the axial steel strains. Strains of transverse steels including spirals and steel plates were also measured with a sufficient number of strain gauges.

## 3. TEST RESULTS AND DISCUSSIONS

### 3.1 Observed Crack Patterns

Fig. 4 displays crack patterns observed at the end of loading. In Fig. 4, the red and blue lines represents the loading in pull and push direction, respectively.

Flexural crack was first observed at  $R=0.0025\text{rad}$  in specimen RS20N33SD reinforced with normal-strength D13 rebars. The width of main flexural crack increased slightly during consecutive loading, and just before  $R$

Table 1 Outlines and primary test results of specimens

Specimen	$a/D$	$f'_c$ (N/mm <sup>2</sup> )	$P$ (kN)	$n$	Longitudinal rebars		Transverse reinforcement			$V_{exp}$ (kN)	$R_{exp}$ (%)	
					Type	$\rho_g$ (%)	Type	$t$ (mm)	$\rho_t$ (%)			$\rho_h$ (%)
RS20N33SD	2	35.1	568.7	0.33	8-D13	2.07	spiral	-	-	2.02	130.0	1.0
RS20N33U	2	36.8	596.3	0.33	8-U12.6	2.03	spiral	-	-	2.02	159.5	5.0
RS40N33T	4	37.0	599.0	0.33	8-U12.6	2.03	plate	1.6	2.56	0.67	89.0	5.0
RS40N50T	4	34.9	857.7	0.50	8-U12.6	2.03	plate	1.6	2.56	0.67	90.8	3.5

Note:  $a/D$  -shear span ratio;  $a$  – shear span of column;  $D$  - cross section diameter of column;  $f'_c$  -concrete compression strength;  $P$  -axial force;  $n$  -axial load ratio;  $\rho_g$  -the ratio of longitudinal rebar;  $t$  -thickness of steel plate;  $\rho_t$  -the volumetric ratio of spirals and hoops;  $\rho_h$  -the volumetric ratio of steel plate;  $V_{exp}$  -ultimate lateral load;  $R_{exp}$  -drift angle at  $V_{exp}$ .

Table 2 Mechanical properties of reinforcement

Name	Type	$f_y$ (N/mm <sup>2</sup> )	$\epsilon_y$ (%)	$f_u$ (N/mm <sup>2</sup> )	$E_s$ (kN/mm <sup>2</sup> )
U12.6*	SBPDN 1275/1420	1357	0.83	1473	215
D13	SD345	354	0.21	413	188
D6	SD295A	366	0.20	484	184
PL1.6	SS400	389	0.19	453	213

Note:  $f_y$  -yield stress;  $f_u$  -tensile strength;  $E_s$  -Young's modulus;  $\epsilon_y$  -yield strain;  $\epsilon^*$  0.2% offset yield strength.

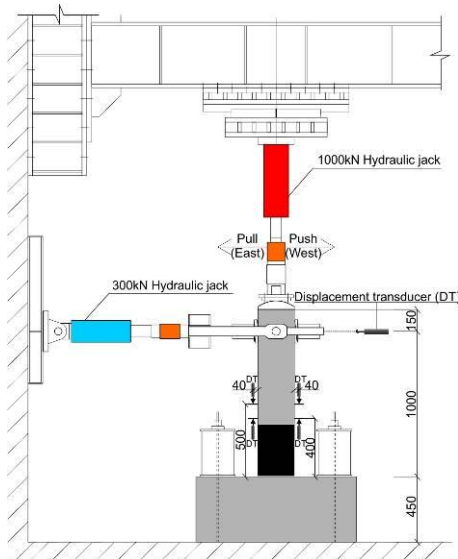
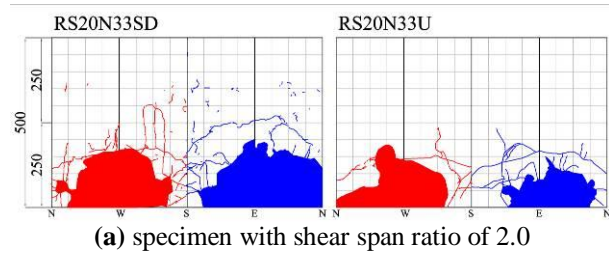


Fig. 3 Schematic view of test setup

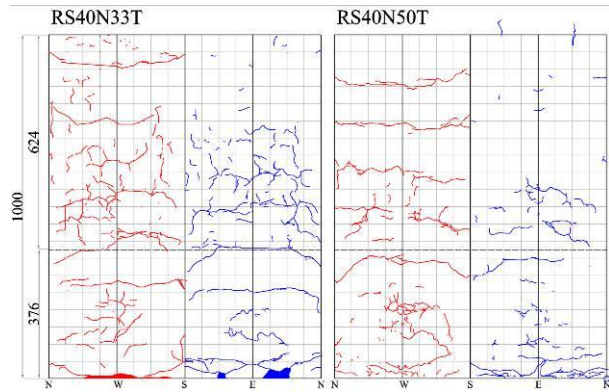
reached 0.015 rad. cover concrete started to spall off. The damaged portion at the end of testing expanded within 250 mm end region of the column as shown in Fig. 4(a).

Specimen RS20N33U with SBPDN rebars exhibited much limited damage until  $R$  was 0.03 rad. The damage concentrated within the end region of about 170mm in length. The cover concrete did not spall off until  $R$  approached 0.025 rad (see Fig. 4(a)).

Crack patterns and damage degree of the two longer columns confined with steel plates were observed after tests by removing the steel plates. As one can see from Fig. 4(b), the damage of these specimens was much minor than observed in the two specimens confined by



(a) specimen with shear span ratio of 2.0



(b) specimen with shear span ratio of 4.0

Fig. 4 Crack patterns

spirals. The steel plates didn't touch the stub until  $R=0.05$  rad.

### 3.2 Lateral Load $V$ Drift Angle $R$ Hysteretic Curves

The lateral load versus drift ratio responses of all specimens are shown in Fig. 5. The solid circles in Fig. 5 locate the experimental maximum load on the curve, while the dashed lines represent the  $P-\Delta$  effect by the axial compression on the lateral resistance.

As can be seen from Fig. 5, the specimens reinforced with SBPDN rebars exhibited very stable and ductile behaviors up to large deformation angle  $R=0.05$  rad. without apparent deterioration in lateral load-carrying capacity even when the axial load ratio was 0.5. On the other hand, the specimen reinforced by normal-strength SD345 rebars exhibited typical ductile behavior up to  $R=0.05$  rad. This column reached its maximum load-carrying capacity at  $R=0.01$  rad where concrete cover commenced spalling off. From that drift ratio on, the lateral resistance of the specimen began to degrade nearly in accordance with the  $P-\Delta$  effect, but still kept about 80% of its maximum lateral resistance at  $R=0.05$

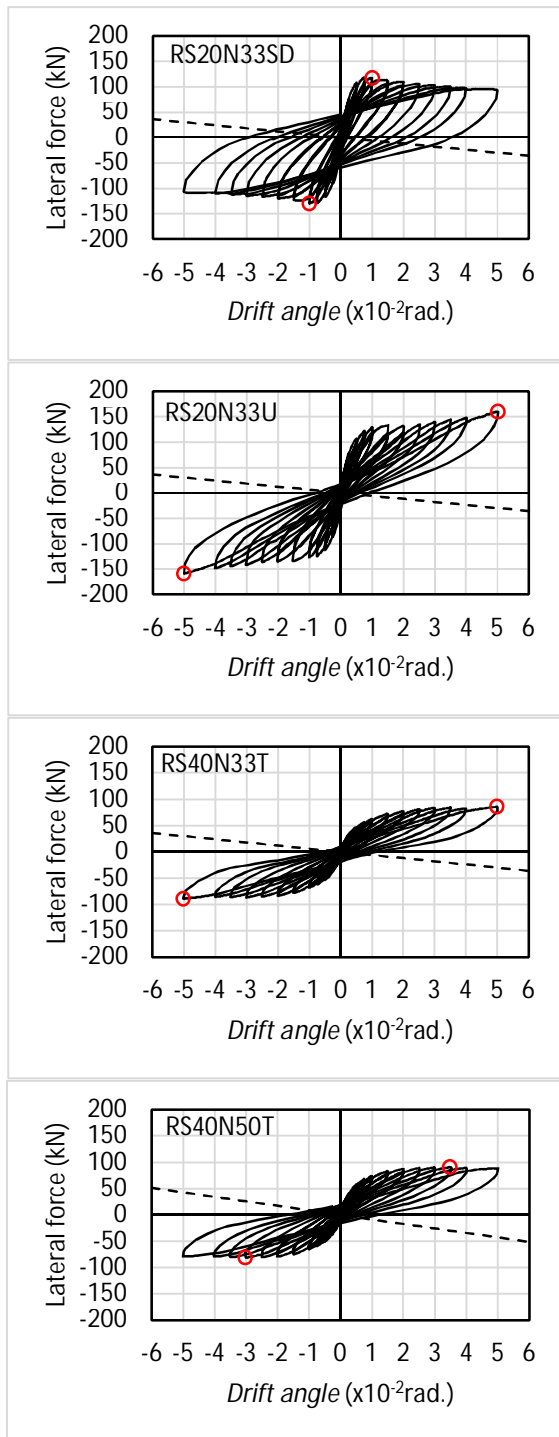


Fig. 5 Measured lateral force V – drift ratio R relationships

rad, which implies high seismic capacity of this specimen from the conventional viewpoint of seismic design with life safety as ultimate goal. On the other hand, negative tangent stiffness at large drift ratio means instability and irreversibility of the column, and causing extremely large drift ratio when the column is hit by a stronger earthquake than anticipated in current seismic design codes and leave a too large residual deformation to be repaired after earthquakes.

To see effectiveness of ultra-high strength rebars in ensuring concrete columns a positive tangent stiffness at large drift level, Fig. 6 compares the moment at the

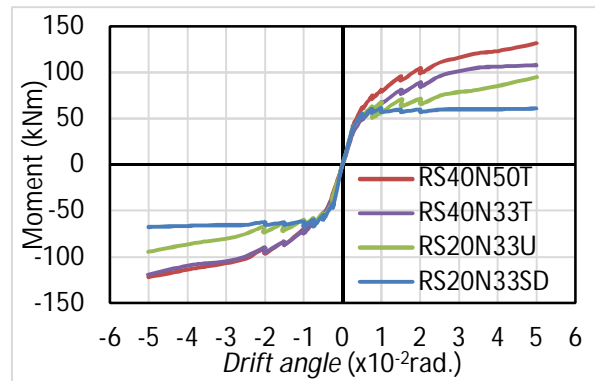


Fig.6 Comparison of moment-drift envelope curves

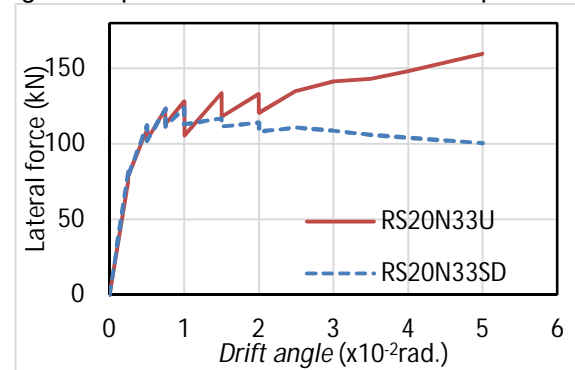


Fig. 7 Effect of type of longitudinal reinforcement

column base versus drift ratio envelope curves of all specimens. The moment shown in Fig. 6 included the P- $\Delta$  moment. It can be seen from Fig. 6 that all specimens reinforced with SBPDR rebars exhibit apparently positive tangent stiffness until large drift in spite of the high axial load level.

The positive tangent stiffness in moment-drift curve until large drift is indispensable to the resilience of concrete columns under severe earthquake, because the increasing moment along with drift will cover the degradation in lateral resistance of the columns due to the P- $\Delta$  effect, assuring the columns of positive tangent stiffness until large drift.

Fig. 7 emphasizes the effect of type of the longitudinal rebars on overall seismic performance of circular concrete columns by comparing the V-R envelope curves of specimens with shear span ratio of 2.0. As can be seen from Fig. 7, both specimens exhibited identical behavior until R reached 0.01 rad. in spite of the difference in steel strength, from that drift on, the lateral resistance of the specimen with SD345 rebars started to degrade along with drift due to the commencement of yielding of longitudinal rebars (see Fig. 8). On the other hand, the lateral resistance of the specimen with SBPDR rebars kept increasing until R reached 0.05 rad without yielding of the SBPDR rebars being observed. Comparison shown in Fig. 7 implies the necessity of keeping rebars in the elastic range if resilient concrete columns are desired.

### 3.3 Strains of longitudinal rebars

Fig. 8 shows the strains of longitudinal rebars measured at the section 25mm away from the column base in both extreme sides of the section. The dashed

horizontal lines represent the yield strain levels of reinforcements. From Fig. 8 one can see that the steel strains of SBPDN rebars did not yield even at  $R=0.05$  rad., but those of SD345 rebars reached their yield strain at the drift ratio of 0.01 rad. The steady increase in the strain of SBPDN rebars along with drift accounted for the increase in steel stress and then the lateral resistance provided by longitudinal rebars. It was this increment in steel strain of SBPDN rebars that covered the loss in lateral resistance caused by the  $P-\Delta$  effect and the inherent degrading property of concrete, enabling the overall lateral resistance of the column to increase along with drift.

Another important phenomenon of the steel strain of SBPDN rebars can be observed from Fig. 9, which illustrates the strain profiles of longitudinal rebars along the column height at several drift levels. The steel strains of SD345 rebars with high bond strength tended to be concentrated at the bottom end of column, while those of SBPDN rebars exhibited expansion from the end region at small drift and to overall height at large drift, finally exhibited almost identical strains along the column height. This observation means that the lower bond strength of SBPDN rebars tends to distribute the strain along the whole length of rebars, avoiding concentration of the steel strain within limited plastic hinge region, mitigating damage degree, and enhancing resilience of concrete columns.

### 3.4 Residual Deformation

Fig.10 shows the measured residual drift angles of all specimens. No difference was observed in the measured residual deformation among specimens with SBPDN and SD345 rebars until  $R$  reached 0.01 rad. After that drift on, the residual drift angle of specimens with SBPDN rebars became much smaller than that of specimen with SD345 rebars. The specimen with higher axial load also showed a slightly larger residual drift angles. The sharp increase of residual drift angle of specimen with SD345 rebars can be attributed to the yielding of the rebars at  $R=0.01$  rad. The residual drift of specimen RS40N50T corresponding to the drift of 0.04 rad was as low as 0.008 rad as compared with the residual drift of 0.023 rad. of specimen RS20N33SD, while the axial load level of the former was higher than that of the latter. This observation implies that partial confinement by steel plates can ensure sufficient resilience until large drift to circular concrete columns under high axial load with axial load ratio of 0.5.

## 4. ANALYSIS OF CYCLIC RESPONSE

Funato et al. have proposed an integrated analytical method to evaluate the hysteresis behavior of concrete members [9]. This method can account for the effect of steel slippage on the cyclic behavior of concrete members and will be adopted to assess the cyclical behavior of the test columns. Fig. 11 shows examples of comparisons between the test and calculated V-R curves. One can see from Fig. 11 that the calculated curve agreed relatively well with the test result of specimen RS20N33U, but underestimated the test result

of specimen RS40N33T. Since the bond strength of  $3 \text{ N/mm}^2$  was proposed in reference 9 based on the pull-out test results of SBPDN rebars in unconfined concrete, the bond strength of SBPDN rebars in the concrete confined by steel plates should be higher than  $3 \text{ N/mm}^2$ . To verify this presumption, the analytical V-R curve of specimen RS40N33T with bond strength of  $5 \text{ N/mm}^2$  for

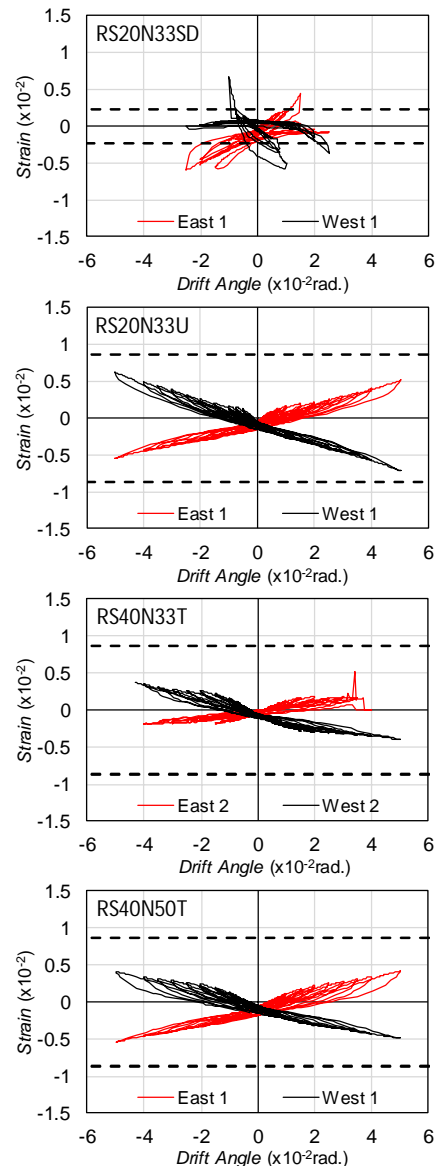


Fig. 8 Strains of longitudinal rebars

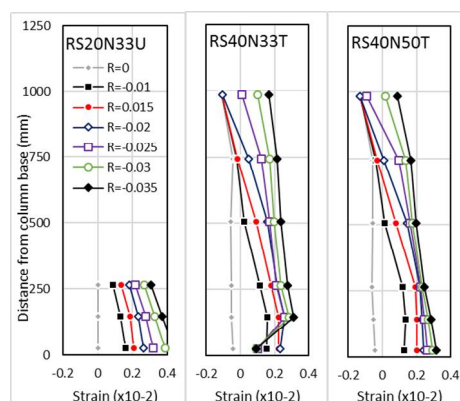


Fig. 9 Strain profiles of longitudinal rebars

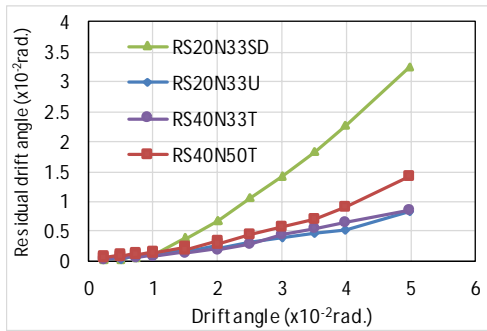


Fig. 10 Measured residual drift ratios

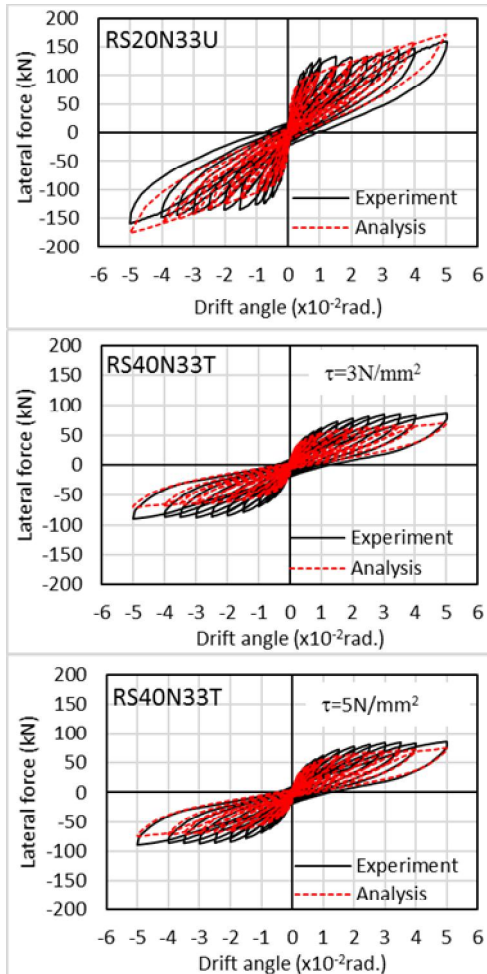


Fig. 11 Comparisons between measured and calculated hysteretic curves

SBPDN rebar is compared with the test one in Fig. 11. As can be seen from Fig. 11, the calculated result with higher bond strength exhibits much better agreement with the test one than initially calculated result.

## 5. CONCLUSIONS

The main conclusions drawn from the studies described in this paper can be summarized as follows.

- (1) Combination of the partial confinement by the bolted steel plates and the use of high strength rebars can ensure circular concrete columns with shear span ratio of 4.0 and under high axial load of sufficient resilience up to large drifts.

- (2) Low bond strength of ultra-high strength SBPDN rebar delays the yielding of longitudinal steels, enhances the secondary stiffness and hence the resilience of concrete columns until large drifts.
- (3) Cyclical behavior of circular concrete columns reinforced by SBPDN rebars can be satisfactorily assessed by the method proposed by Funato et al. To improve accuracy of analysis for the columns confined by steel plates, the bond-strength of SBPDN rebars should be increased to  $5\text{N/mm}^2$ , which needs further analytical investigation and testing.

## ACKNOWLEDGEMENT

The support received from Neturen Co. Ltd, which provided ultra-high strength SBPDN rebars, and the help from Mr. Masaru KANAO during the testing are gratefully acknowledged.

## REFERENCES

- [1] Sun, Y., et al. "Stress-strain relationships of high-strength concrete confined by circular steel tubes." Transactions of the Japan Concrete Institute, 21:3, 601-606, 1999. (in Japanese)
- [2] Xiao, Y., and Hui, Wu, H. "Retrofit of reinforced concrete columns using partially stiffened steel jackets." J. Struct. Eng., ASCE, 129(6), 725-732, 2003
- [3] Sun, Y. "Ultimate Strength Equations for R/C Members Retrofitted by Circular Steel Tubes." Proc. of the 4th International Conference on Urban Earthquake Engineering, Tokyo, 245-250, 2007.
- [4] Choi, E., Chung, Y., Park, J., and Cho, B. "Behavior of reinforced concrete columns confined by new steel-jacketing method." ACI Struct. J., 107(6), 654-662, 2010.
- [5] Sun Y., Cai G. and Takeuchi T. "Seismic Behavior and Performance-Based Design of Resilient Concrete Columns", International Journal of Applied Mechanics and Materials, Vols. 438-439, pp. 1453-1460, 2013.
- [6] Wang J., Takeuchi T., Koyama T. and Sun Y. "Seismic behavior of circular fly ash concrete column reinforced by ultra-high strength rebars and steel plates." Proceedings of the Japan Concrete Institute, 36(2), 115-120, 2014.
- [7] Sargsyan G et al. "Experimental study on seismic behavior of resilient circular concrete columns." Proceedings of the Japan Concrete Institute, 37(2), 187-192, 2015. (in Japanese)
- [8] Cai G et al., "Seismic performance of circular RC columns using low bond high strength rebars." Proceedings of the Japan Concrete Institute, 35(2), 145-150., 2013. (in Japanese)
- [9] Funato Y., Sun Y., Takeuchi T. and CAI G. "Modeling and application of bond characteristic of high-strength reinforcing bar with spiral grooves." Proceedings of the Japan Concrete Institute, 34(2), 157-162, 2012. (In Japanese)
- [10] Architectural Institute of Japan, "AIJ Standards for Structural Calculation of Reinforced Concrete Structures", Maruzen, Tokyo, 2010. (in Japanese)